Design wave identification using different hydrodynamic models

Athanasios Dermatis, Seung-Yoon Han, Sylvain Jamet, Benjamin Bouscasse, Guillaume Ducrozet
Nantes Université, École Centrale Nantes, CNRS, LHEEA, UMR 6598, Nantes, France
Email: athanasios.dermatis@ec-nantes.fr

1 INTRODUCTION

The design wave approach is one of the most promising alternatives to the Monte Carlo approach in irregular waves for estimating the short-term response distribution of offshore structures [1]. Design waves are typically employed within a multi-fidelity framework, in which a simple and computationally efficient low-fidelity model is first used to obtain a preliminary response distribution, as illustrated in Figure 1. For several target probability levels P_{tar}, the same model is then used to identify wave events that induce the corresponding target response χ_{tar}. The wave episodes are subsequently reproduced using a high-fidelity model, such as experiments or CFD simulations, and the resulting peak response χ_{NL} is finally used to revise the preliminary response distribution at P_{tar}. According to classification societies [1], suitable design wave candidates can be derived using so-called response-conditioning methods. The concept of conditional wave episodes was introduced by the NewWave model [2] and later extended to derive response-conditioned waves (RCWs) through the Most Likely Extreme Response method [3]. These approaches provide closed-form expressions for the most probable wave elevation and response profiles, making them highly practical. However, they rely on the assumption of an underlying linear wavefield and a linear response amplitude operator (RAO). As a result, when these wave episodes are reproduced in experiments or CFD simulations, nonlinear wave-wave interactions can lead to significant discrepancies in the generated wave patterns. Moreover, the use of RAO limits their applicability to configurations that can be adequately described by linear frequency-domain analysis. In this work, a recently proposed method [4] is employed to overcome the limitations of these traditional approaches by explicitly accounting for nonlinear wave propagation within a numerical wave tank (NWT). In addition, response conditioning is performed through the solution of an optimisation problem, similar to the First-Order Reliability Method (FORM) [5]. The performance of the design wave approach is investigated for the platform motions of a spar-type floating offshore wind turbine (FOWT), using linear, second-order, and time-domain models in the response conditioning procedure.

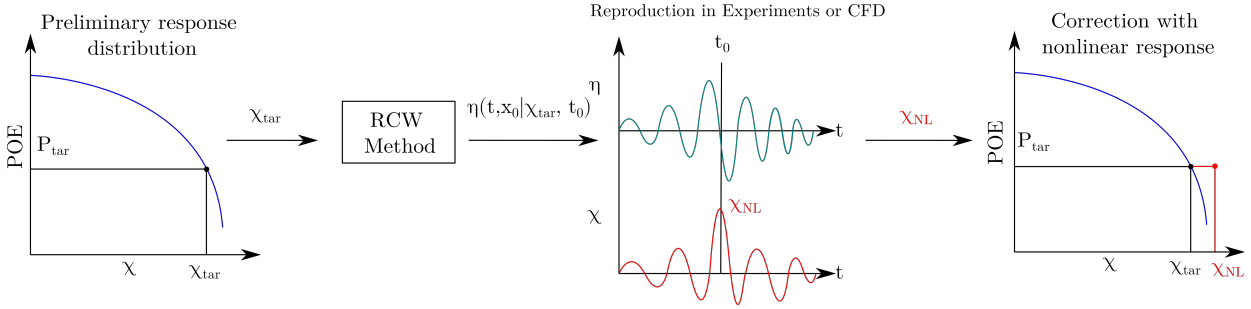

Figure 1: Schematic overview of multi-fidelity design wave methodology

2 NONLINEAR RESPONSE CONDITIONING

A limit state function is considered as the difference between the target response level χ_{tar} and the response $\chi(t_0)$ at the target time instant t_0,

$$G(\mathbf{u}) = \chi_{tar} - \chi(t_0|\mathbf{u}) = 0 \tag{1}$$

where, $\mathbf{u} = \{u_1, \bar{u}_1, ..., u_N, \bar{u}_N\}$ is a vector of uncorrelated standard normal variables. Instead of expressing the wave elevation in a vector form, as done for a linear wavefield, the nonlinear wave propagation is considered in a numerical wave tank [6], and the wavemaker is described by,

$$X_{wm}(t) = \sum_{n=1}^{N} \frac{A_n}{L^{wm}(\omega_n)} \cos\,\omega_n t = \sum_{n=1}^{N} (u_n c_n(t) + \bar{u}_n \bar{c}_n(t)) \tag{2}$$

$$c_n(t) = \sigma_n^{wm} \cos\,\omega_n t \qquad \bar{c}_n(t) = -\sigma_n^{wm} \sin\,\omega_n t \qquad (\sigma_n^{wm})^2 = \frac{S_\eta(\omega_n)}{(|L^{wm}(\omega_n)|)^2} \Delta\omega_n \tag{3}$$

where ω_n is the wave frequency, A_n is the complex wave amplitude determined by the wave spectrum $S_\eta(\omega_n)$, and $L^{wm}(\omega_n)$ is the wavemaker transfer function. Then, the wave propagation is solved by the `HOS-NWT` solver [6], and the wave elevation $\eta^{HOS}(x,t)$ is provided. A response $\chi(t)$, based on frequency-domain analysis, can be reconstructed at first or second order as,

$$\chi(t) = \chi^{(1)}(t) = \sum_{n=1}^{N} \hat{X}^{(1)}(\omega_n) \alpha_n e^{\mathrm{i}\omega_n t} \tag{4}$$

$$\chi(t) = \chi^{(1)}(t) + \chi^{(2)}(t) = \sum_{n=1}^{N} \hat{X}^{(1)}(\omega_n) \alpha_n e^{\mathrm{i}\omega_n t} + \sum_{m=1}^{N} \sum_{n=1}^{N} \hat{X}^{(2)}(\omega_m, \omega_n) \alpha_m \alpha_n^{\pm} e^{\mathrm{i}(\omega_m \pm \omega_n)t} \tag{5}$$

where $\hat{X}^{(1)}$ is the complex RAO and $\hat{X}^{(2)}$ is the response quadratic transfer function (QTF). In addition, α_n is the complex wave amplitude at the structure location x_0, obtained from the Fourier Transform of the nonlinear wave elevation $\eta^{HOS}(x_0, t)$, and $\alpha_n^{\pm}$ denotes the use of the complex conjugate if the difference-frequency QTF is used. Alternatively, $\eta^{HOS}(x_0, t)$ can be directly inserted in time-domain simulations of arbitrary nonlinearity to obtain $\chi(t)$. Overall, different sets of $\mathbf{u}$ yield different realisations of the wavemaker motion, and thus, wave episodes, which are translated to responses through the chosen expression for $\chi(t)$. The identification of the RCW is then performed by solving the following FORM-based optimisation procedure [4, 5],

$$\min \sqrt{\sum_{n=1}^{N} (u_n^2 + \bar{u}_n^2)} \quad \text{subject to} \quad G(\mathbf{u}) = \chi_{tar} - \chi(t_0|\mathbf{u}) = 0 \tag{6}$$

3 RESULTS

In this study, a spar-type FOWT was investigated experimentally at a scale of 1/40. The floater was flexible and identical to the one presented in [7], designed to carry the DTU 10MW turbine. Frequency domain analysis was performed using `Hydrostar` [8] to obtain the RAO and the QTF for the platform motions. The resulting hydrodynamic database, consisting of the linear and quadratic excitation force transfer functions, was also used in time-domain simulations performed with `OpenFAST` [9]. Therefore, three different low-fidelity models were considered as surrogates for the response-conditioning procedure, and the main elements of each model are outlined in Table 1.

Table 1: Different hydrodynamic models used for response conditioning

Method	**Response**	**Model**	**Mooring**
Linear	Equation (4)	RAO	Linear stiffness
Second-order	Equation (5)	RAO+QTF^{-}	Linear stiffness
Time-domain	`OpenFAST`	RAO+QTF$^{\pm}$+Morison	Quasi-static (MAP++)

Two unidirectional sea states were considered for the analysis, described by a Pierson-Moskowitz spectrum, and their features are given in Table 2. For each sea state, 20 irregular wave realisations

were generated experimentally in the absence of wind, corresponding to a total duration of 2 hours at full scale. Empirical response distributions were then derived from these realisations, within a Monte Carlo approach, and are used as a benchmark to assess the accuracy of the design wave approach. Moreover, for the first step of the methodology, the preliminary distribution was obtained as the Rayleigh distribution for the linear model. For the other two models, it was empirically constructed through numerical Monte Carlo Simulations (MCS) [10]. Regarding the RCW, the target conditional values for the heave and pitch motions were selected according to the Rayleigh distribution for the target probability levels $P_{tar} = [0.1, 0.01, 0.005, 0.001]$. For the surge motion, they were set as multiples of the standard deviation $\chi_{tar} = [\sigma_{\xi_1}, 2\sigma_{\xi_1}, 3\sigma_{\xi_1}, 4\sigma_{\xi_1}]$ of the total first- and second-order response spectrum. When the target probability level is not explicitly specified, it can be determined by interpolating the target response levels in the preliminary distribution.

Table 2: Description of environmental conditions (full scale)

Case	H_s (m)	T_p (s)	IW Realisations	RCW Tests
SS5	5.5	13	20'× 20	1'× 4/response
SS15	15.6	15.2	20'× 20	1'× 4/response

Figure 2 presents the results for the surge, heave and pitch exceedance probability distributions of SS5. The empirical Monte Carlo distribution of the experimental responses is denoted as 'Exp. MCS', while the respective distribution obtained with the second-order model is denoted as 'Quad. MCS'. In addition, the results of the experimental design wave tests with linear RCW are labelled as 'Lin. RCW', and for the tests with second-order RCW as 'Quad RCW'. The same results for SS15 are presented in Figure 3, where 'Opf. MCS' is the preliminary distribution obtained by `OpenFAST` simulations, and 'Opf. RCW' are the corresponding design wave high-fidelity results. The results suggest that the design wave approach, using linear RCW, falls short in capturing the fully nonlinear responses when those are not primarily driven by linear hydrodynamics. For the milder sea state, the inclusion of second-order effects provides results that closely follow the experimental Monte Carlo distribution. For the severe case of SS15, the frequency-domain model and `OpenFAST` provide comparable results for surge and heave motions. However, for the pitch motion, only the time-domain RCWs provide good estimates of the experimental distribution. Figure 4 presents a comparison between the RCW free-surface profiles determined by each model for the most extreme wave episode of SS15. It is shown that, especially for the heave motion, the inclusion of second-order effects substantially influences the wave episode obtained.

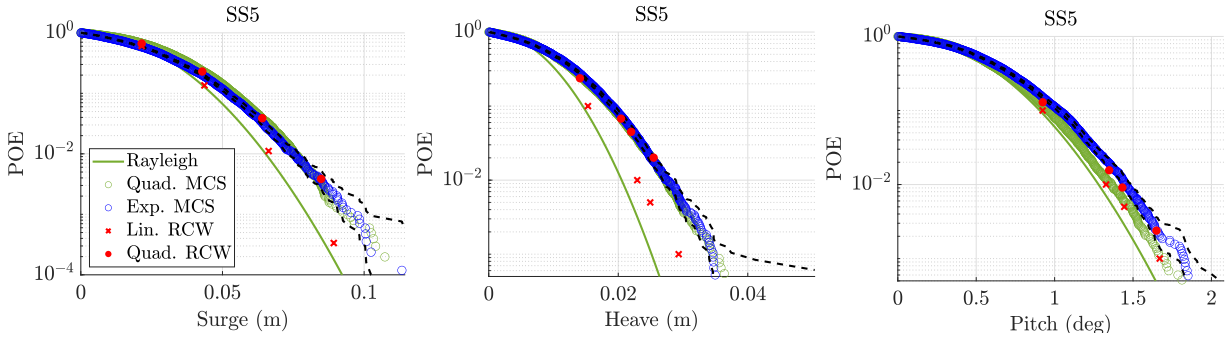

Figure 2: Surge (left), heave (middle), and pitch (right) motion distributions for SS5

4 CONCLUSIONS

Overall, the present study demonstrates that linear RCWs, despite being widely used, are ineffective in capturing the statistics of several hydrodynamic responses of floating offshore wind tur-

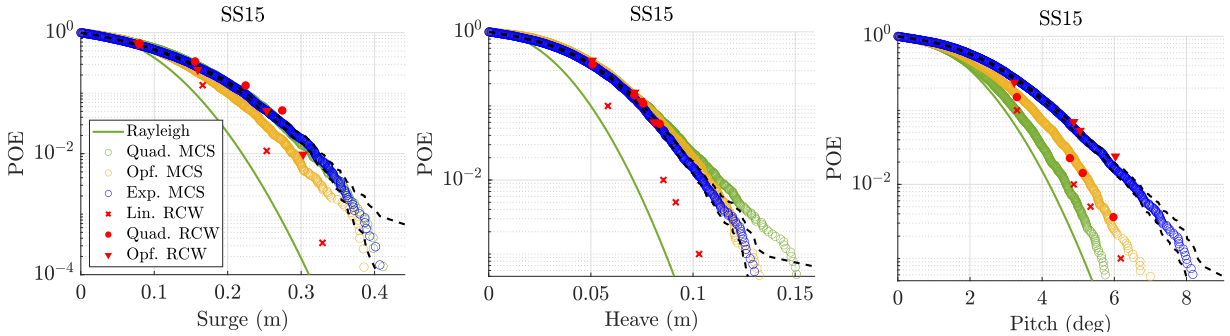

Figure 3: Surge (left), heave (middle) and pitch (right) motion distribution for SS15

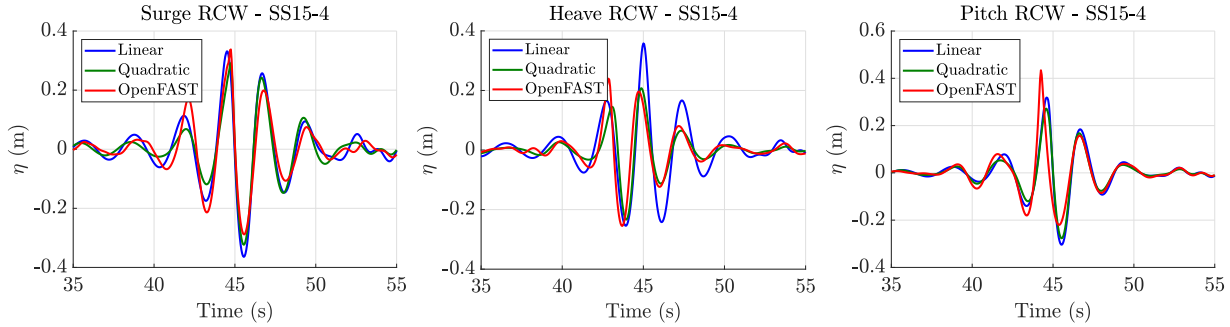

Figure 4: Comparison of RCW profiles for the most extreme wave episodes of SS15

bines. The problem is treated by considering also the QTF in the response conditioning procedure, or time-domain simulations that include the second-order wave loads. Such use of time-domain models, despite being computationally intensive, paves the way for several promising topics, such as determining design waves under the combined action of wind and waves.

This research was supported by the FLOATFARM project, funded by the European Union's Horizon Europe programme (Grant Agreement No. 101136091).

REFERENCES

[1] Bureau Veritas. 2019. *Guidance for long-term hydro-structure calculations.*

[2] Tromans, P. S., Anaturk, A. R., and Hagemeijer, P. A New Model For The Kinematics Of Large Ocean Waves-Application As a Design Wave. In *1st ISOPE* (1991).

[3] Adegeest, L. J. M., Braathen, A., and Vada, T. Evaluation of methods for estimation of extreme nonlinear ship responses based on numerical simulations and model tests. In *22nd SNH* (1998).

[4] Dermatis, A., Lasbleis, M., Kim, S., De Hauteclocque, G., Bouscasse, B., and Ducrozet, G. 2025. *A multi-fidelity approach for the evaluation of extreme wave loads using nonlinear response-conditioned waves. Ocean Eng. 316.*

[5] Jensen, J. J., and Capul, J. 2006. *Extreme response predictions for jack-up units in second order stochastic waves by FORM. Probabilistic Eng. Mech. 21.*

[6] Ducrozet, G., Bonnefoy, F., Le Touzé, D., and Ferrant, P. 2012. *A modified High-Order Spectral method for wavemaker modeling in a numerical wave tank. Eur. J. Mech. B Fluids 34*, 19–34.

[7] Leroy, V., Delacroix, S., Merrien, A., Bachynski-Polic, E. E., and Gilloteaux, J. C. 2022. *Experimental investigation of the hydro-elastic response of a spar-type floating offshore wind turbine. Ocean Engineering 255.*

[8] Chen, X. 2007. *Middle-field formulation for the computation of wave-drift loads. J. Eng. Math. 59*, 61–82.

[9] Jonkman, J. 2007. *Dynamics Modeling and Loads Analysis of an Offshore Floating Wind Turbine.* PhD thesis, University of Colorado at Boulder.

[10] Dermatis, A., Bouscasse, B., Ducrozet, G., Bredmose, H., and Bingham, H. B. 2025. *Prediction of the extreme slow-drift response of moored floating structures using design waves. Ocean Eng. 333.*